PROCEEDINGS OF SCIENCE

Precision Measurements of Neutral Pion Electroproduction Near Threshold: A Test of Chiral QCD Dynamics

R. Lindgren[*a], **K. Chirapatimol**[a], **L. C. Smith**[a] **and Hall A Collaboration.**
[a] *University of Virginia, Charlottesville, VA.*
E-mail: ral5q@virginia.edu,khem@virginia.edu,lcs1h@virginia.edu

Preliminary results are presented from an experiment to measure π^0 electroproduction at and above threshold using the $p(e,e'p)\pi^0$ reaction. The data were taken at a beam energy of 1192 MeV using a two-spectrometer setup in Hall A at Jefferson Lab. For the first time in π^0 threshold electroproduction, complete coverage of the ϕ^*_π and θ^*_π angles in the center-of-mass (C.M.) was obtained for the invariant mass region up to ΔW=18 MeV above the π^0 threshold. At the same time our invariant momentum transfer squared covers the range $Q^2 = 0.05 - 0.15$ (GeV/c)^2 with twelve bins in Q^2. The improved kinematic coverage in C.M., W and Q^2 will better constrain theoretical interpretations of the data using phenomenological models and QCD-inspired models such as Heavy Baryon Chiral Perturbation Theory.

The 7th International Workshop on Chiral Dynamics,
August 6 -10, 2012
Jefferson Lab, Newport News, Virginia, USA

[*]Speaker.

PoS(CD12)073

1. Introduction

The study of neutral pion photo- and electroproduction at threshold provides an important test of the leading order corrections to soft pion theorems predicted by Heavy Baryon Chiral Perturbation Theory (HBCHPT) [1], a low-energy expansion of QCD in which the internal structure of pions and hadrons is systematically incorporated into Low Energy Constants (LEC), while the long-wavelength external dynamics are fixed by PCAC and chiral symmetry. Once the LECs are determined by experiment at threshold, parameter free predictions of the energy dependence of the reaction can be confronted with data. Experimental determination of the energy range over which the LECs do not vary can help establish the convergence of the chiral expansion.

Results from 20 years of increasingly precise π^0 photoproduction cross section and photon asymmetry Σ data have determined the $s-$ and $p-$wave multipoles and their LECs and examined the region of convergence of the chiral expansion. The most recent analysis of MAMI CB-TAPS data compared to fits of $O(q^4)$ HBCHPT shows good agreement for invariant masses up to ΔW=25 MeV above threshold [2, 3], although the reported LECs disagree somewhat with previous estimates [4].

Further insight can be obtained through electroproduction experiments, where the Q^2 dependence of the $s-$wave multipoles E_{0+} and L_{0+} is strongly constrained by gauge invariance and a soft-pion theorem. Polarization observables can also help constrain the LECs. Up to now, only limited multipole analyses from the experimental groups have been published [5, 6, 7], and the combined results from several MAMI experiments showed a Q^2 dependence [7] at threshold incompatible with HBCHPT. The most recent MAMI experiment [8] reported total cross sections for three Q^2 points within 4 MeV of threshold, but a refit of HBCHPT to these data has not been published. The JLab experiment reported here will provide the most extensive data set to date for threshold π^0 electroproduction.

2. Formalism

Under the one-photon-exchange approximation, the $p(e,e'p)\pi^0$ cross section factorizes as follows:

$$\frac{d^3\sigma}{dQ^2 dW d\Omega_\pi^*} = J\Gamma_v \frac{d\sigma}{d\Omega_\pi^*}, \tag{2.1}$$

where Γ_v is the virtual photon flux and the Jacobian $J = \partial(Q^2,W)/\partial(E_{e'}, cos\,\theta_{e'}, \phi_{e'})$ relates the differential volume element of data binned in the invariants dQ^2dW to the scattered electron kinematics $dE_{e'}\,dcos\,\theta_{e'}\,d\phi_{e'}$. For unpolarized beam and target the center-of-mass (C.M.) differential cross section $d\sigma$ depends on the transverse ε and longitudinal ε_L polarization of the virtual photon through the response functions: R_T, R_L and their interference terms R_{LT} and R_{TT}:

$$\frac{d\sigma}{d\Omega_\pi^*} = \frac{p_\pi^*}{k_\gamma^*}(R_T + \varepsilon_L R_L + \varepsilon R_{TT}\sin^2\theta_\pi^*\cos 2\phi_\pi^* + [2\varepsilon_L(\varepsilon+1)]^{1/2} R_{LT}\sin\theta_\pi^*\cos\phi_\pi^*), \tag{2.2}$$

where $(p_\pi^*, \theta_\pi^*, \phi_\pi^*)$ are the π^0 C.M. momentum, polar, and azimuthal angles. Note ϕ_π^* defines the rotation of the $p\pi^0$ plane with respect to the electron scattering plane (e,e'). Other definitions are $\varepsilon_L = (Q^2/|k^*|^2)\varepsilon$, $\Gamma_v = \alpha/2\pi^2(E'/E)(k_\gamma/Q^2)(1-\varepsilon)^{-1}$ and $J = \pi W/EE'm_p$ where $|k^*|$ and k_γ^* are the virtual photon C.M. momentum and real photon C.M. equivalent energy.

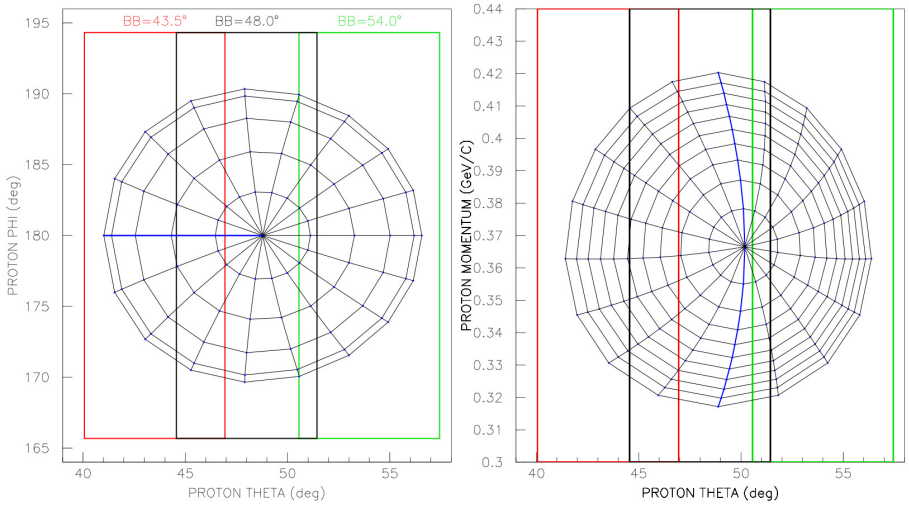

Figure 1: Left: Overlap between BigBite Spectrometer proton laboratory angle acceptance (colored boxes) and $p\pi^0$ center-of-mass bins at Q^2=0.135 (GeV/c)^2 and ΔW=9.5 MeV. Radial and concentric lines separate bins of ϕ_π^* and θ_π^* respectively. Only 5 out of 9 θ_π^* bins are shown. Blue line shows ϕ_π^*=180. Right: Radial and concentric lines separate bins of θ_π^* and ΔW respectively projected onto lab momentum p_p and θ_p. Bins to the (left,right) of the blue line correspond to (ϕ_π^*=180°, ϕ_π^*=0°). Innermost circle is ΔW = 0.5 MeV.

3. Experiment

The $p(e,e'p)\pi^0$ experiment was performed in Hall A at Jefferson Lab using the Left High Resolution Spectrometer (LHRS) [9] to detect the scattered electron and the BigBite spectrometer (BB) [10] to detect the coincident proton. The CEBAF polarized beam was energy locked to 1192.38 MeV and delivered to a 6 cm long 2.54 cm wide cylindrical liquid Hydrogen (LH2) target. Beam currents below 5 μA were used to prevent target boiling and reduce the singles rates in the LHRS. Four angle settings for LHRS ($\theta_{e'}$=12.5°,14.5°,16.5° and 20.5°) covered a nearly continuous invariant momentum transfer range of Q^2=0.05-0.15 (GeV/c)^2 using a 4.4 msr acceptance cut. The LHRS momentum bite was centered on the $p\pi^0$ threshold and covered the range -3% $< \delta p/p <$ +5%. Three angle settings for BB (θ_p=43.5°,48.0° and 54.0°) provided 100% coverage of the proton cone up to an invariant mass of ΔW=18 MeV above the $p\pi^0$ threshold at the highest Q^2 due to the large BB angular acceptance (Fig. 1). The BB central momentum was set at 0.38 GeV/c, while momentum acceptance was limited by target energy loss at low momentum ($p_p < 0.25$ GeV) and thresholds on the $E-\Delta E$ scintillator counters at high momentum ($p_p > 0.5$ GeV). The low momentum cutoff was achieved using a thin (1 mil) Ti exit window in the target scattering chamber and a helium bag for transport up to and between the BB drift chambers. Absolute normalization, energy and angle calibration in both spectrometers were checked at each kinematic setting using elastic scattering runs with LH2 and thin solid targets.

Selection of the $p\pi^0$ final state required trigger particle identification in both spectrometers and determination of the missing mass M after reconstruction of the detected particle's 3-momenta:

$$M^2 = (E + m_p - E_{e'} - E_p)^2 - (\vec{p}_e - \vec{p}_{e'} - \vec{p}_p)^2. \tag{3.1}$$

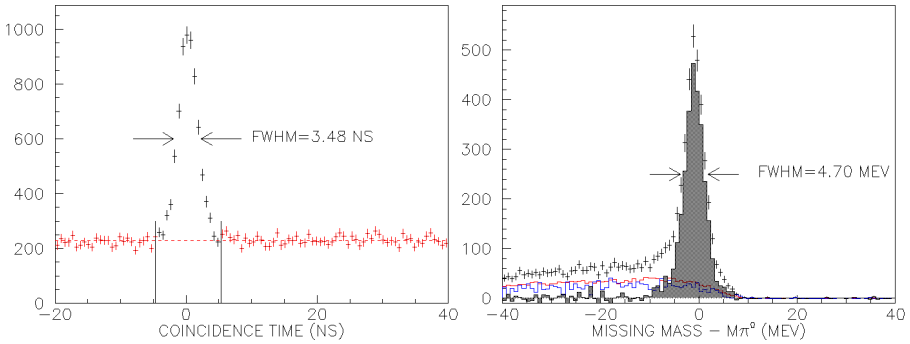

Figure 2: Left: Coincidence timing between LHRS and BB. Events belonging to the true coincidence peak were selected using the vertical line cuts, while random coincidences were selected using the region highlighted in red. Right: Missing mass distribution at Q^2=0.15 (GeV/c)^2 for the invariant mass range 1073.25<W<1083.25 MeV. Background events from random coincidences (red) and target cell windows (blue) were subtracted form the raw distribution, leaving the π^0 missing mass peak shown in gray.

Scintillator hodoscopes provided the primary trigger for both spectrometers. An additional gas threshold Cěrenkov detector in the LHRS provided electron identification with 99% efficiency. Signals from either E or ΔE scintillator planes at the rear of BB made the coincidence trigger. A combination of $E - \Delta E$ cuts on the highly segmented scintillators, combined with drift chamber signal thresholds which vetoed minimum ionizing tracks, completely suppressed charged pion tracks in BigBite. The pathlength corrected coincidence time distribution between LHRS and BB is shown in Fig. 2. A 10 ns wide cut centered on the peak was used to select true coincidences, while a 60 ns cut (excluding the peak) selected random coincidences. The experimental missing mass distribution is also shown in Fig. 2 before and after subtraction of both random coincidences and target window contributions. The latter background was estimated using cuts on ΔW below the π^0 threshold, and is dominated by quasi-free $\gamma^* n \to p\pi^-$ production from the aluminum windows.

Before calculation of the kinematics required for binning the data, the scattered electron was corrected for ionization energy losses in exiting the target, while the incident beam energy was corrected to reflect the actual energy at the target interaction vertex. Radiative straggling losses were incorporated into the Monte Carlo simulations. Proton transport energy losses through the target and BigBite were also corrected for each event. The background subtracted yield was normalized to luminosity and various detector inefficiencies and an acceptance correction derived from Monte-Carlo simulations of both spectrometers was applied, using the DMT model as a physics event generator. Special care was taken to incorporate into the simulations the measured energy and angular resolution and energy calibration determined from elastic scattering runs, in order to properly account for their systematic effects near threshold.

4. Preliminary Results

Events were accumulated in 18 ϕ_π^* and 9 θ_π^* bins for each Q^2 and W bin using cuts of $\pm$10 MeV on the missing mass peak. The data were binned at 1 MeV intervals in ΔW. The average Q^2 binwidth was 0.01 (GeV/c)^2. Fig. 3 shows typical differential cross sections for each ϕ_π^* and θ_π^* bin

obtained at Q^2=0.135 (GeV/c)^2 and ΔW = 9.5 MeV. The curve labeled BKM96 is the HBCHPT prediction from Bernard, Kaiser and Meisner [1] based on LECs which were determined by fits to older photoproduction data from MAMI and electroproduction data at Q^2=0.1 (GeV/c)^2 from MAMI and NIKHEF. The other curve is an empirical fit to the data which we use to obtain the total cross section σ_{tot}. This fit, which uses the form in Eq.(2.2) and assumes the structure functions are dominated by $s-$waves and $p-$waves, does a reasonable job of fitting the data.

The Q^2 dependence of σ_{tot} is shown in Fig. 4 for different ΔW bins starting 0.5 MeV above threshold. Only statistical errors are shown. The overall systematic error at threshold is believed to be less than 15%. The BKM96 fit is also shown along with phenomenological models (DMT, MAID [11], SAID [12]) which have been fitted to the world data on pion photo- and electroproduction. It is observed that the slope of our measurement of σ_{tot} at the lower Q^2 values over the entire ΔW range shown here is more consistent with the BKM96 predictions of heavy baryon chiral perturbation theory than those of the phenomenological models. At higher Q^2 values, the opposite is true. The slope of the measurement of σ_{tot} is more consistent with predictions of the phenomenological models. It would be of interest to refit the BKM96 LECs to our data and compare to the results recently reported for photoproduction [2] to see if the leading order LECs are consistent. This would help resolve the question of whether the Q^2 evolution seen in our data reflects the need for higher order LECs to describe the poorly converging $s-$wave expansion or whether only a simple readjustment of the single $p-$wave LEC is needed.

In summary, our new measurement of the total cross section for threshold π^0 electroproduction extends the coverage of previous experiments and provide a clearer view of both the Q^2 and W evolution of this process. Further partial wave analysis and extraction of the multipoles will help to address the question of the convergence of the chiral expansion used in HBCHPT.

References

[1] V. Bernard, N. Kaiser, Ulf-G. Meiβner, Nucl. Phys. A **607** (1996) 379.

[2] C. Fernandez-Ramierex and A.M. Bernstein, arXiv:1212.3237.

[3] D. Hornidge et al. and CB@MAMI Collaboration, arXiv:1211.5495.

[4] V. Bernard et al., Eur. Phys. J. A **11** (2001) 209.

[5] H.B. van den Brink et al., Nucl. Phys. A **612** (1997) 391.

[6] M.O. Distler et al., Phys. Rev. Lett. **80** (1998) 2294.

[7] H. Merkel et al., Phys. Rev. Lett. **88** (2002) 012301-1.

[8] H. Merkel et al., arXiv:1109.5075.

[9] J. Alcorn et al., Nucl. Instr. and Meth. A **522** (2004) 294.

[10] M. Mihovilovic et al., Nucl. Inst. and Meth. A **686** (2012) 20.

[11] MAID07 and DMT solutions obtained from: http://wwwkph.kph.uni-mainz.de/MAID/. See also D. Drechshel, S.S. Kamalov, and L. Tiator, Eur. Phys. J. A **34**, 69 (2007); S.S. Kamalov and S.N. Yang, Phys. Rev. Lett. **83**, 4494 (1999).

[12] R.A. Arndt et al., Chinese Phys. C **33**, 1063 (2009) and SAID website: http://gwdac.phys.gwu.edu.

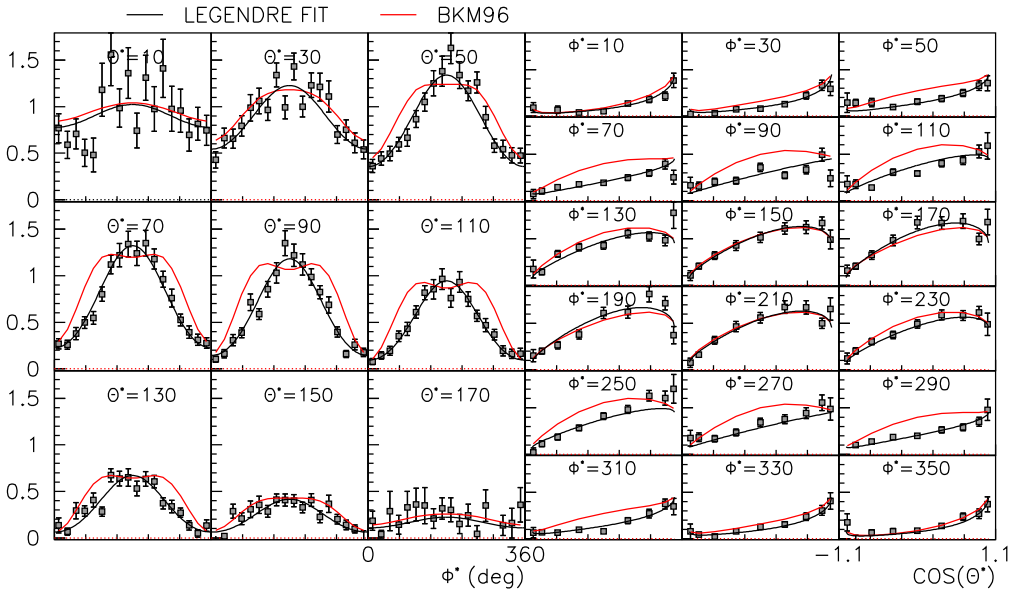

Figure 3: Preliminary differential cross sections at Q^2 = 0.135 (GeV/c)^2 and ΔW = 9.5 MeV from this experiment binned in $p\pi^0$ center-of-mass variables ϕ^*_π and and cosθ^*_π. See text for description of curves. Errors are statistical only.

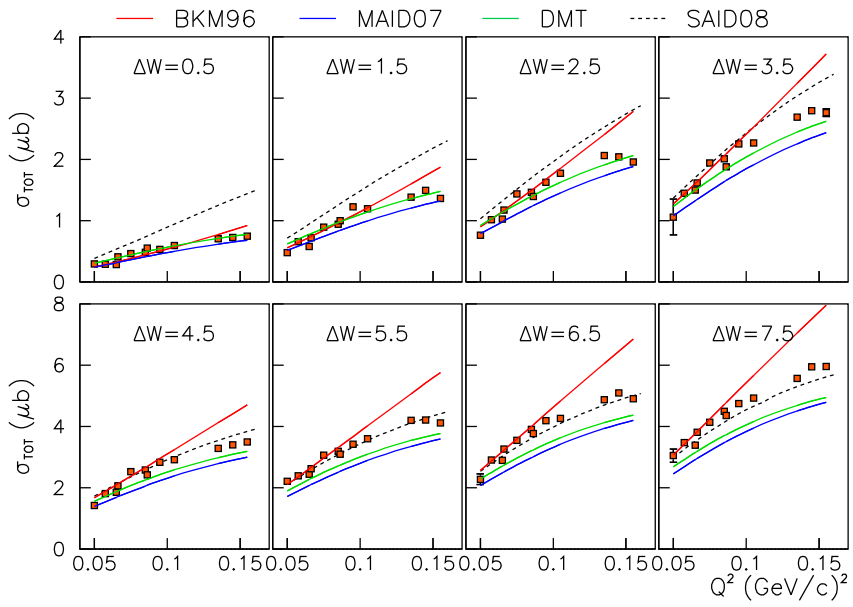

Figure 4: Preliminary results for Q^2 dependence of π^0 electroproduction total cross section for different bins of ΔW, the invariant mass above threshold. Units of ΔW are MeV. Errors are statistical only. Model curves are described in the text.